THE JOURNAL OF BIOLOGICAL CHEMISTRY VOL. 289, NO. 8, pp. 5285–5295, February 21, 2014

Ankyrin-B Regulates $Ca_v2.1$ and $Ca_v2.2$ Channel Expression and Targeting*

Received for publication, October 1, 2013, and in revised form, December 30, 2013 Published, JBC Papers in Press, January 6, 2014, DOI 10.1074/jbc.M113.523639

Crystal F. Kline[‡1], John Scott[‡], Jerry Curran[‡], Thomas J. Hund[§], and Peter J. Mohler[‡¶‖]

From the [‡]Dorothy M. Davis Heart and Lung Research Institute, the Departments of [¶]Physiology and Cell Biology and [‖]Internal Medicine, The Ohio State University Wexner Medical Center, and the [§]Department of Biomedical Engineering, College of Engineering, The Ohio State University, Columbus, Ohio 43210

Background: Calcium channels control membrane excitability. The mechanisms underlying $Ca_v2.1$/$Ca_v2.2$ targeting are not well understood.
Results: Ankyrin-B associates with $Ca_v2.1$/$Ca_v2.2$. Loss of ankyrin-B results in reduced expression of $Ca_v2.1$/$Ca_v2.2$ in select brain regions.
Conclusion: Ankyrin-B plays a role in the expression of $Ca_v2.1$/$Ca_v2.2$.
Significance: Results identify pathway for membrane targeting of calcium channels and regulation of membrane excitability.

N-type and P/Q-type calcium channels are documented players in the regulation of synaptic function; however, the mechanisms underlying their expression and cellular targeting are poorly understood. Ankyrin polypeptides are essential for normal integral membrane protein expression in a number of cell types, including neurons, cardiomyocytes, epithelia, secretory cells, and erythrocytes. Ankyrin dysfunction has been linked to defects in integral protein expression, abnormal cellular function, and disease. Here, we demonstrate that ankyrin-B associates with $Ca_v2.1$ and $Ca_v2.2$ in cortex, cerebellum, and brain stem. Additionally, using *in vitro* and *in vivo* techniques, we demonstrate that ankyrin-B, via its membrane-binding domain, associates with a highly conserved motif in the DII/III loop domain of $Ca_v2.1$ and $Ca_v2.2$. Further, we demonstrate that this domain is necessary for proper targeting of $Ca_v2.1$ and $Ca_v2.2$ in a heterologous system. Finally, we demonstrate that mutation of a single conserved tyrosine residue in the ankyrin-binding motif of both $Ca_v2.1$ (Y797E) and $Ca_v2.2$ (Y788E) results in loss of association with ankyrin-B *in vitro* and *in vivo*. Collectively, our findings identify an interaction between ankyrin-B and both $Ca_v2.1$ and $Ca_v2.2$ at the amino acid level that is necessary for proper $Ca_v2.1$ and $Ca_v2.2$ targeting *in vivo*.

Neurons are highly polarized cells, where structural, functional, and molecular differences within the neuronal physiology underlie the ability to receive, process, and transmit information. The specific expression profile of ion channels, receptors, and cytoskeletal proteins present within select neuronal membrane domains plays a primary role in defining local function of the entire cell. Recently, studies focused on the role of cytoskeletal proteins in the genesis and maintenance of local membrane domains in excitable cells have revealed a new and exciting avenue of study for these proteins in physiology and disease (1, 2).

Calcium ions are critical second messengers involved in the regulation of multiple neuronal cellular processes, but primarily synaptic transmission (3–7). Ca^{2+} entry across the plasma membrane occurs via voltage-dependent calcium channels (VDCCs).[2] To maintain the tight spatio-temporal distribution of intracellular Ca^{2+} necessary to mediate a diverse array of functions, VDCCs have evolved with respect to their biophysical properties, regulation, and subcellular localization (8). The physiological importance of VDCCs is further exemplified by the variety of mutations in VDCC channel components linked to neurological and motor diseases (9). VDCCs have been classified into five groups, identified as T, L, N, P/Q, and R, based on electrophysiological and pharmacological properties (9–12). N- and P/Q-type currents are observed primarily in neurons and co-localize with a subset of docked vesicles at the synapse, where they control exocytosis (13–15) and initiate synaptic neurotransmission (3, 4, 16). VDCCs are heteromultimers composed of the pore-forming $\alpha 1$ subunit and associated auxiliary subunits, $Ca_v\beta$ and $\alpha 2\delta$ (for review, see Ref. 4). Although auxiliary subunits have been demonstrated to enhance $\alpha 1$B expression (17, 18), the mechanisms underlying Ca_v channel membrane expression and localization are not clearly defined.

Ankyrins are a class of membrane adaptor proteins necessary for the targeting and regulation of select membrane and cytoplasmic proteins (19). In the brain, ankyrin-G is a necessary component for the functional organization of initial segments and nodes of Ranvier. Targeted disruption of cerebellar ankyrin-G results in severe ataxia, loss of ability to fire action potentials, and loss of $Na_v1.6$ from the initial segment (20, 21). Additionally, there is loss of nodal β_{IV} spectrin and KCNQ2/3 channels with indiscriminate localization of the cell adhesion

* This work was supported, in whole or in part, by National Institutes of Health Grants HL084583, HL083422, and HL114383 (to P. J. M.) and HL096805 and HL114893 (to T. J. H.). This work was also supported by the American Heart Association (to P. J. M.), the Saving Tiny Hearts Society (to P. J. M.), and The Ohio State University William D. and Jacquelyn L. Wells Fund for Cardiovascular Research (to P. J. M.).

[1] To whom correspondence should be addressed: Dorothy M. Davis Heart and Lung Research Institute, 473 W. 12th Ave., DHLRI 110G, Columbus OH 43210. Tel: 614-292-5019; Fax: 614-247-7799; E-mail: faith.kline@osumc.edu.

[2] The abbreviations used are: VDCC, voltage-dependent calcium channel; ABM, ankyrin-binding motif; CTD, C-terminal domain; IP, immunoprecipitation; MBD, membrane-binding domain; SBD, spectrin-binding domain.

molecule neurofascin (21, 22). Loss of neurofascin expression at the initial segment of Purkinje neurons results in disruption of interneuron synapses connecting Purkinje neurons in the cerebellum (23). Likewise, ankyrin-B has been demonstrated to play a critical role in the establishment and maintenance of excitable domains in brain (24). Loss of ankyrin-B in mice results in significant nervous system defects, including hypoplasia of the corpus callosum and pyramidal tracts, dilation of the lateral ventricles, and deterioration of long axon tracts (25). Notably, recent work outside of the brain has defined new roles for ankyrin-B for targeting select voltage-gated Ca^{2+} channels in the pacemaking cells of the cardiac sinoatrial node (26, 27). We therefore tested the role of ankyrin-B for targeting select calcium channels in the brain.

Our findings define a role for ankyrin-B in neuronal cell biology by demonstrating ankyrin-B-dependent interactions that are required for proper $Ca_v2.1$ and $Ca_v2.2$ expression in brain. We observed a significant decrease in $Ca_v2.1$ and $Ca_v2.2$ expression in cortex, cerebellum, and brain stem tissues of ankyrin-B-deficient mice. In defining the structural requirement for this interaction, we demonstrate that the ankyrin-B membrane-binding domain associates directly with $Ca_v2.1$ and $Ca_v2.2$. Specifically, this interaction occurs in the DII/III loop region of both VDCCs. Finally, a single amino acid mutation at residue Tyr-797 in $Ca_v2.1$ and Tyr-788 in $Ca_v2.2$ is sufficient to disrupt association of ankyrin-B with $Ca_v2.1$ or $Ca_v2.2$. Collectively, our data demonstrate a necessary role for ankyrin-B in the expression of $Ca_v2.1$ and $Ca_v2.2$ in brain.

EXPERIMENTAL PROCEDURES

Animals—Mice were age-matched wild-type, ankyrin-$B^{+/-}$, and ankyrin-G cerebellar-specific knock-out littermates. Animals were backcrossed at least 20 generations (99.8% pure) into the C57BL/6 background (Jackson Laboratories). Ankyrin-G cerebellar-specific knock-out mice were generated as described (25). Animals were handled according to approved protocols and animal welfare regulations of the Institutional Animal Care and Use Committee at Ohio State University. All mice were housed and handled identically.

Antibodies—The following primary antibodies were used for immunoblotting and/or immunostaining: anti-ankyrin-B (polyclonal), anti-ankyrin-G (polyclonal), anti-$Ca_v2.2$ (polyclonal; Thermo Scientific and Alomone Labs), anti-$Ca_v2.1$ (polyclonal; Alomone Labs); anti-GAPDH (monoclonal; Fitzgerald Industries International); anti-GFP (NeuroMabs). Secondary antibodies used for immunoblotting were HRP-conjugated donkey anti-rabbit (Jackson Laboratories) and HRP-conjugated donkey anti-mouse (Jackson Laboratories). Secondary antibody used for immunostaining were Alexa Fluor 568 goat anti-rabbit Ig (Invitrogen). $Ca_v2.1$ and $Ca_v2.2$ antibodies were validated using immunoblots from HEK293 cells transfected with either GFP-$Ca_v2.1$ or GFP-$Ca_v2.2$. $Ca_v2.1$ Ig specifically recognized GFP-$Ca_v2.1$, but not GFP-$Ca_v2.2$. Conversely, $Ca_v2.2$ Ig specifically recognized GFP-$Ca_v2.2$, but not GFP-$Ca_v2.1$.

$Ca_v2.1$ and $Ca_v2.2$ Constructs—Primers were designed to clone amino acids 708–1194 ($Ca_v2.1$ DII/DIII loop), 788–1194, and 808–1194 from rat full-length $Ca_v2.1$ cDNA based on the sequence obtained from GenBank (NM_012918.3). To facilitate subcloning into pcDNA3.1$^+$, primers were designed to incorporate 5′ EcoRI and 3′ XhoI restriction sites. To facilitate subcloning into pEGFP-C3, primers were designed to incorporate 5′ EcoRI and 3′ BamHI restriction sites. Full-length $Ca_v2.1$ constructs were generated from rat $Ca_v2.1$. To facilitate subcloning into pAcGFP1-N2, primers were designed to incorporate 5′ HindIII and 3′ SalI restriction sites. Primers were designed to clone amino acids 710–1139 ($Ca_v2.2$ DII/III loop), 779–1139, and 799–1139 from a murine brain cDNA library based on the sequence obtained from GenBank (NM_001042528). To facilitate subcloning into pcDNA3.1$^+$ (Invitrogen), primers were designed to incorporate 5′ EcoRI and 3′ XhoI restriction sites. To facilitate subcloning into pEGFP-C3 (Clontech), primers were designed to incorporate 5′ EcoRI and 3′ BamHI restriction sites. Full-length $Ca_v2.2$ constructs were generated from rat $Ca_v2.2$. To facilitate subcloning into pAcGFP1-N2, primers were designed to incorporate 5′ SalI and 3′ KpnI restriction sites. All sequences were verified prior to experiments.

Site-directed Mutagenesis—Primers designed to insert the Y788E mutation into the $Ca_v2.2$ DII/III loop in pcDNA3.1$^+$ and pEGFP-C3 and the full-length $Ca_v2.2$ in pAcGFP1-N2 or the Y797E in $Ca_v2.1$ DII/III loop in pcDNA3.1$^+$ and pEGFPC3 and the full-length $Ca_v2.1$ in pAcGFP1-N2 were used in concert with the Stratagene QuikChange Site-directed Mutagenesis kit and manufacturer's instructions. All sequences were verified prior to experiments.

In Vitro Translation/Binding—$Ca_v2.1$ and $Ca_v2.2$ constructs were *in vitro* translated using rabbit reticulocyte lysate, [^{35}S]methionine (20 μCi of Redivue L-[^{35}S]methionine; GE Healthcare), T7 polymerase, and 0.63 ng of plasmid DNA (TNT Coupled Rabbit Reticulocyte Lysate System; Promega). For binding experiments, 20 μg of purified GST, ankyrin-B membrane-binding domain (MBD)-GST, ankyrin-B spectrin-binding domain (SBD)-GST, or ankyrin-B C-terminal domain (CTD)-GST was coupled to glutathione-Sepharose for 2 h at 4 °C in IV Binding Buffer (50 mM Tris-HCl (pH 7.35), 1 mM EDTA, 1 mM EGTA, 150 mM NaCl, 0.1% Triton X-100). Following extensive washing in IV Wash Buffer (50 mM Tris-HCl (pH 7.35), 1 mM EDTA, 1 mM EGTA, 350 mM NaCl, 0.1% Triton X-100), conjugated beads were incubated with $Ca_v2.1$ or $Ca_v2.2$ *in vitro* translated products overnight at 4 °C in IV Wash Buffer. The beads were washed five times in IV Wash Buffer, eluted, and separated by SDS-PAGE. Gels were stained with Coomassie Blue to show the presence of GST proteins before drying the gel (Bio-Rad Laboratories). Radiolabeled proteins were detected by phosphorimaging or standard autoradiography.

Tissue Preparation and Homogenization—For immunoblot and co-immunoprecipitation (co-IP) analysis, brain tissues (cortex, cerebellum, and brain stem) were flash-frozen in liquid nitrogen and ground into a fine powder. The powder was resuspended in 2 volumes of ice-cold homogenization buffer (50 mM Tris-HCl (pH 7.35), 10 mM NaCl, 0.32 M sucrose, 5 mM EDTA, 2.5 mM EGTA, 1 mM PMSF, 1 mM AEBSF, 10 μg/ml leupeptin, and 10 μg/ml pepstatin) and homogenized using a hand-held homogenizer (27, 28). The homogenate was centrifuged at 1000 $\times$ *g* at 4 °C to remove nuclei. Triton X-100 and deoxycholate were added to the postnuclear supernatant for final concentrations of 0.75% Triton X-100 and 1% deoxycholate.

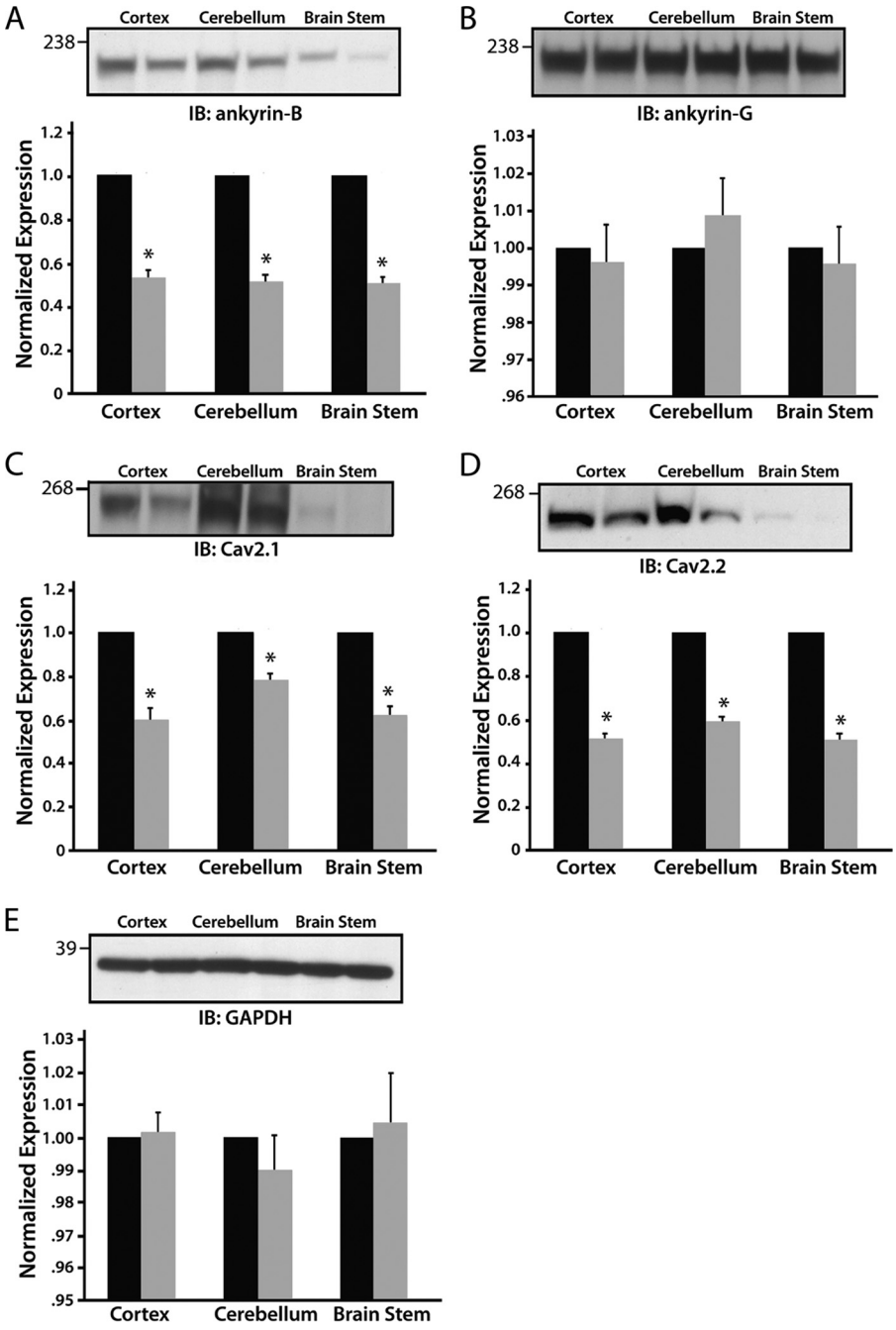

FIGURE 1. **$Ca_v2.1$ and $Ca_v2.2$ expression levels are decreased in ankyrin-$B^{+/-}$ brain lysates.** Ankyrin-B, $Ca_v2.1$, and $Ca_v2.2$ expression levels are significantly decreased in cortex, cerebellum, and brain stem in ankyrin-$B^{+/-}$ mice compared with wild-type mice (*A*, *C*, and *D*, respectively). There are no significant differences in expression between wild-type and ankyrin-$B^{+/-}$ lysates of ankyrin-G (*B*) or GAPDH (*E*, loading control). For each *panel*, $n = 4$ for each genotype ($p < 0.05$).

The lysate was pelleted at high speed for 15 min at 4 °C. The resulting supernatant was quantitated by bicinchoninic acid assay prior to analysis.

Immunoblots—Immunoblots from anti-ankyrin-B, anti-$Ca_v2.1$, anti-$Ca_v2.2$, and anti-ankyrin-G blots were evaluated by densitometry and expression normalized to anti-GAPDH blots (29, 30). Histograms represent expression as a percentage of wild-type expression (wild-type expression normalized to 100%).

Tissue Preparation for Immunostaining—Freshly extracted tissues from wild-type and ankyrin-$B^{+/-}$ mice were fixed in 4% paraformaldehyde for 12 h and the tissues transferred to 10, 20, and 30% sucrose solutions for 12 h each. Tissues were cryosectioned to 10-μm thickness. Cryosections were rehydrated in PBS prior to preblocking in 3 mg/ml BSA in PBS. Primary antibodies were made in a vehicle of 3 mg/ml BSA with 0.1% Triton X-100 in PBS and incubated on sections overnight at 4 °C. The slides were washed three times in vehicle and incubated with Alexa Fluor donkey anti-rabbit 568 secondary antibodies for 3 h at 4 °C. Following three washes in vehicle, the slides were mounted with VectaShield (Vector Laboratories) and no. 1 coverslips. Images were collected on a Zeiss 510 Meta confocal microscopy using Carl Zeiss software.

Co-IP from Brain Lysates—Protein A-conjugated agarose beads (AffiGel; Bio-Rad) were incubated with either control Ig or anti-Ca_v2.2 Ig, anti-Ca_v2.1 Ig, or anti-ankyrin-B Ig in co-IP binding buffer (PBS with 0.1% Triton X-100 and protease inhibitor mixture (Sigma)) for 12 h at 4 °C. Beads were centrifuged and washed three times in ice-cold PBS. Wild-type cortex, cerebellum, or brain stem tissue lysate were added to the washed beads, along with protease inhibitor mixture and co-IP binding buffer, and incubated for 12 h at 4 °C. The reactions were washed three times in ice-cold co-IP buffer. The samples were eluted and the proteins separated by SDS-PAGE prior to immunoblots with ankyrin-B, Ca_v2.1, or Ca_v2.2 Ig. Experiments were performed multiple times with similar results. Due to the low copy number of Ca_v2.1 and Ca_v2.2 in brain regions, lysate inputs were scaled up. For experiments where Ca_v2.1 or Ca_v2.2 Igs were immobilized on beads, 1 mg of cortex and cerebellum lysate was used, whereas 2 mg of brain stem lysate was used. Input lanes represent 10% of total lysate used. For experiments where ankyrin-B Ig was immobilized on beads, 1 mg of lysate for each brain region was utilized. Input lanes represent 5% of total lysate for cortex and cerebellum and 10% of total lysate for brain stem.

Co-IP from Transfected Cells—Protein A-conjugated agarose beads were incubated with either control IgG or affinity-purified anti-ankyrin-B Ig for 12 h at 4 °C. Beads were centrifuged and washed three times in ice-cold PBS. 100 μg of transfected HEK lysate was added to the washed beads, along with protease inhibitor mixture and IP buffer, and incubated for 12 h at 4 °C. The reactions were washed three times in ice-cold IP buffer. The samples were eluted and the proteins separated by SDS-PAGE prior to immunoblots with anti-GFP Ig. For co-IP using full-length calcium channel-transfected cells, input lanes represent 20% of total lysate input (400 μg). For GFP-Ca_v channel loop transfections, input lanes represent 10% of total lysate input (200 μg).

Pulldowns—One hundred micrograms of wild-type cortex, cerebellum, or brain stem lysate was added to 10 μg of GST, GST-ankyrin-B MBD, GST-ankyrin-B SBD, or GST-ankyrin-B CTD-conjugated beads, along with 500 μl of Binding Buffer, protease inhibitor mixture (Sigma), and PMSF. The reactions incubated for 12 h at 4 °C. The beads were centrifuged and washed three times in binding buffer. The proteins were eluted, separated by SDS-PAGE, and immunoblotted using anti-Ca_v2.1 Ig and anti-Ca_v2.2 Ig.

HEK293 Cell Culture and Transfection of Ca_v2.1 and Ca_v2.2 Fragments—HEK293 cells were maintained in Dulbecco's modified essential medium (Invitrogen) supplemented with 10% fetal bovine serum (FBS; HyClone) and 0.1% penicillin/streptomycin. Cells were cultured at 37 °C in 5% CO_2. Cultured cells were split 24 h prior to transfection and plated to obtain 30% confluence at time of transfection. Effectene reagent (Qiagen) was used to transfect cells with 0.2 μg Ca_v2.2 DII/III pEGFP-C3, Ca_v2.2 DII/III Y788E pEGFP-C3, or pEGFP-C3 alone. Transfection was carried out for 7 h at 37 °C and the cells recovered overnight. After 48 h, the cells were fixed with 2% paraformaldehyde, stained with ToPro (to discriminate nuclear material), and evaluated by confocal microscopy. Likewise, transfections using Ca_v2.1 DII/III pEGFP-C3, Ca_v2.1 DII/III Y797E pEGFP-C3, and pEGFP-C3 alone were also performed using the same protocol.

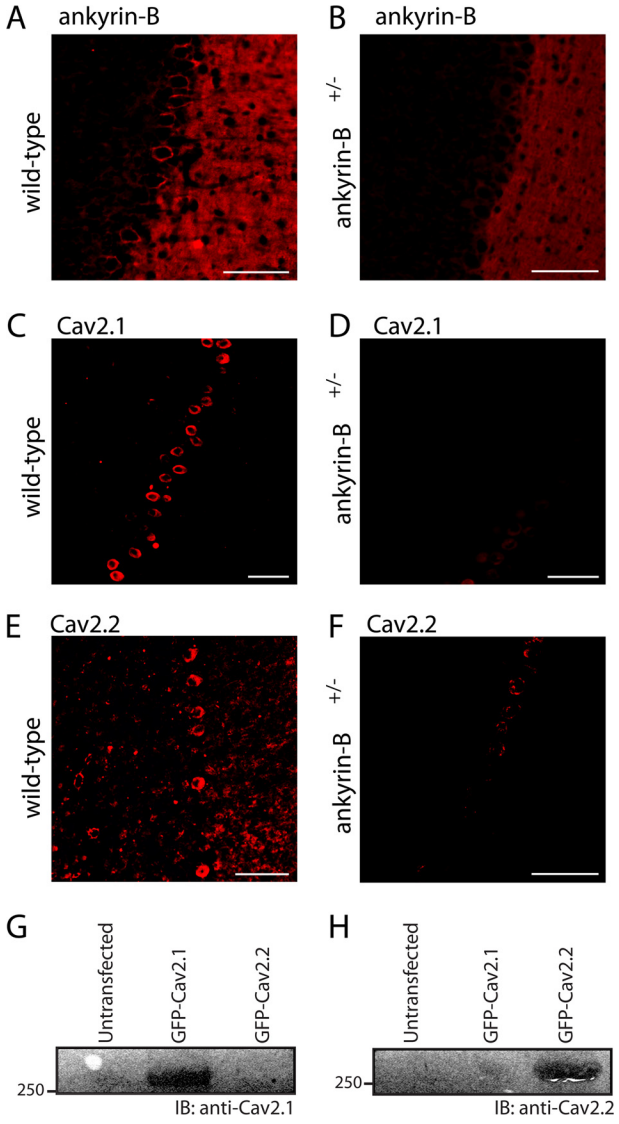

FIGURE 2. **Ankyrin-B$^{+/-}$ mice display a significant decrease in ankyrin-B, Ca_v2. 1, and Ca_v2.2 expression in cerebellar Purkinje neurons.** *A* and *B*, ankyrin-B expression is significantly reduced in ankyrin-B$^{+/-}$ Purkinje neurons. Note that ankyrin-B is expressed in both Purkinje cell layer and molecular layer. *C–F*, Ca_v2.1 (*C* and *D*) and Ca_v2.2 (*E* and *F*) expression is significantly reduced in the Purkinje neurons of ankyrin-B$^{+/-}$ mice. *Scale bar* denotes 20 μm. *G* and *H*, Ca_v2.1 and Ca_v2.2 antibodies are validated. Untransfected HEK293 cells and HEK293 cells transfected with either full-length GFP-Ca_v2.1 or GFP-Ca_v2.2 were analyzed by co-immunoprecipitation or immunoblotting (*IB*). In *G*, Ca_v2.1 Ig recognizes GFP-Ca_v2.1 but not GFP-Ca_v2.2. In *H*, Ca_v2.2 Ig recognizes GFP-Ca_v2.2 but not GFP-Ca_v2.1.

HEK293 Cell Culture and Transfection for Confocal Microscopy—HEK293 cells were maintained in Dulbecco's modified essential medium supplemented with 10% FBS and 0.1% penicillin/streptomycin. Cells were cultured at 37 °C in 5% CO_2. Cultured cells were split 24 h prior to transfection and plated on MatTek plates to obtain 90% confluence at time of transfection. Lipofectamine (Invitrogen) was used to transfect cells with 1 μg of Ca_v2.2-GFP, 1 μg of Ca_v2.2 Y788E-GFP, 1 μg of Ca_v2.1-GFP, 1 μg of Ca_v2.1 Y797E-GFP, or pAcGFP1-N2 alone. Transfection was carried out for 5 h at 37 °C and the cells recovered overnight. After 24 h, the cells were fixed with 2% paraformal-

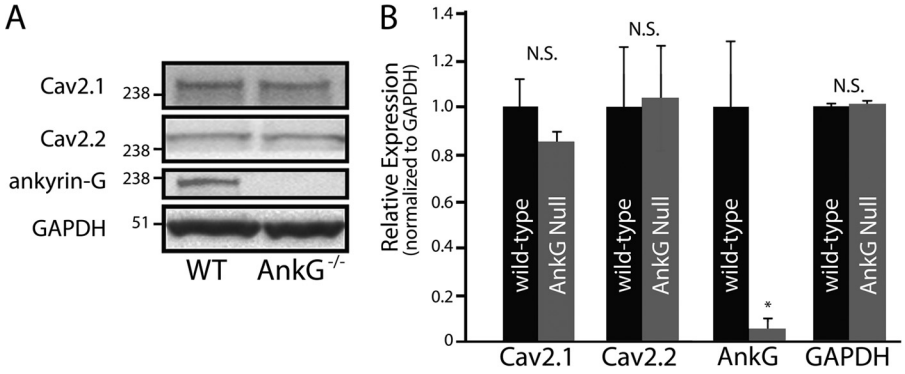

FIGURE 3. **Ankyrin-G is not required for $Ca_v2.1$ or $Ca_v2.2$ expression.** Although ankyrin-G cerebellar-specific knock-out mice display a significant reduction in the expression of ankyrin-G (*A*), there are no significant differences in the expression of $Ca_v2.1$ or $Ca_v2.2$ between wild-type and ankyrin-G cerebellar-specific knock-out cerebellar lysates (*A* and *B*, $n = 4$; *N.S.*). Ankyrin-G levels by immunoblotting in ankyrin-G cerebellar-specific knock-out mice were significantly reduced and similar to background.

dehyde, mounted with VectaShield (with DAPI), and evaluated by confocal microscopy.

HEK293 Cell Culture and Transfection for Co-immunoprecipitations—HEK293 cells were maintained in Dulbecco's modified essential medium supplemented with 10% FBS and 0.1% penicillin/streptomycin. Cells were cultured at 37 °C in 5% CO_2. Cultured cells were split 24 h prior to transfection and plated on 100-mm^2 plates to obtain 90% confluence at time of transfection. Lipofectamine (Invitrogen) was used to transfect cells with 1 μg of $Ca_v2.2$-GFP, 1 μg of $Ca_v2.2$ Y788E-GFP, 1 μg of $Ca_v2.1$-GFP, 1 μg of $Ca_v2.1$ Y797E-GFP, or pAcGFP1-N2 alone. Untransfected cells were used as a negative control. Transfection was carried out for 5 h at 37 °C and the cells recovered overnight. After 24 h, the cells were lysed in IP buffer (25 mM Tris-HCl (pH 7.4), 150 mM NaCl, 1 mM EDTA, 1% Nonidet P-40, 5% glycerol, protease inhibitor mixture (Sigma)) and centrifuged to remove cellular debris, and the protein was quantitated by bicinchoninic acid assay (Pierce).

Statistics—Data are presented as a mean ± S.D., and statistical significance was assessed using Student's *t* test. The null hypothesis was rejected for $p < 0.05$.

RESULTS

$Ca_v2.1$ and $Ca_v2.2$ Expression Is Reduced in Ankyrin-$B^{+/-}$ Brain—Ankyrins are key players for targeting ion channels in excitable cells. Recent work defined new roles for ankyrin-B for targeting select voltage-gated Ca^{2+} channels in the pacemaking cells of the cardiac sinoatrial node (26, 27). We therefore tested the role of ankyrin-B for targeting select calcium channels in the nervous system. Specifically, we investigated $Ca_v2.1$ and $Ca_v2.2$ subunit expression in ankyrin-$B^{+/-}$ cortex, cerebellum, and brain stem. As expected, ankyrin-B expression was significantly reduced in ankyrin-$B^{+/-}$ cortex, cerebellum, and brain stem lysates (Fig. 1*A*; decreased 53, 52, and 51%, respectively; $n = 4$, $p < 0.0001$), whereas the expression levels of the related ankyrin gene product, ankyrin-G (Fig. 1*B*), and GAPDH (loading control; Fig. 1*E*) were unchanged. We observed decreased $Ca_v2.1$ expression in cortex (41%), cerebellum (20%), and brain stem (35%) in ankyrin-$B^{+/-}$-derived tissues compared with wild-type lysates (Fig. 1*C*; $n = 4$, $p < 0.05$). $Ca_v2.2$ expression was also reduced in ankyrin-$B^{+/-}$ cortex (49%), cerebellar (40%), and brain stem tissue (50%) compared with lysates from wild-type littermates (Fig. 1*D*; $n = 4$, $p < 0.05$).

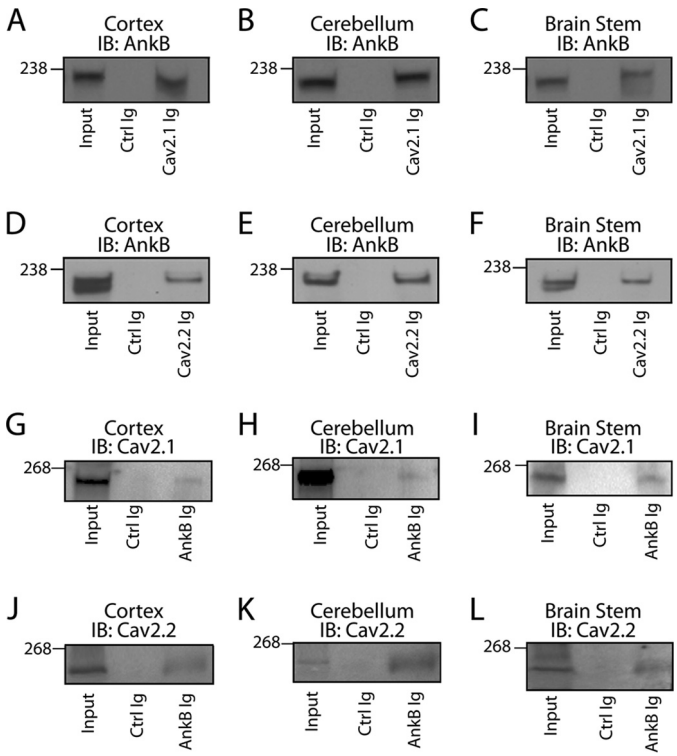

FIGURE 4. **Ankyrin-B co-immunoprecipitates with $Ca_v2.1$ and $Ca_v2.2$.** *A–F*, $Ca_v2.1$ Ig and $Ca_v2.2$ Ig co-immunoprecipitate ankyrin-B from detergent-soluble lysates of cortex (*A* and *D*), cerebellum (*B* and *E*), and brain stem (*C* and *F*), respectively. No significant interaction was observed with control (*Ctrl*) Ig. *G–L*, ankyrin-G Ig co-immunoprecipitates $Ca_v2.1$ and $Ca_v2.2$ from detergent-soluble lysates of cortex (*G* and *J*), cerebellum (*H* and *K*), and brain stem (*I* and *L*), respectively. No significant interaction was observed with control Ig. *IB*, immunoblotting.

Based on our immunoblot findings, we performed confocal analysis for the localization of $Ca_v2.1$ and $Ca_v2.2$ in wild-type and ankyrin-$B^{+/-}$ mouse cerebellum. In the cerebellum, $Ca_v2.1$ and $Ca_v2.2$ are expressed in Purkinje neurons and localized in the cell body (31, 32). Ankyrin-B is also expressed in the cerebellar Purkinje neuron cell body, as well as throughout the molecular layer (33). As shown in Fig. 2, whereas ankyrin-B, $Ca_v2.1$, and $Ca_v2.2$ are robustly expressed in Purkinje neurons from wild-type cerebellum, we observed a significant decrease

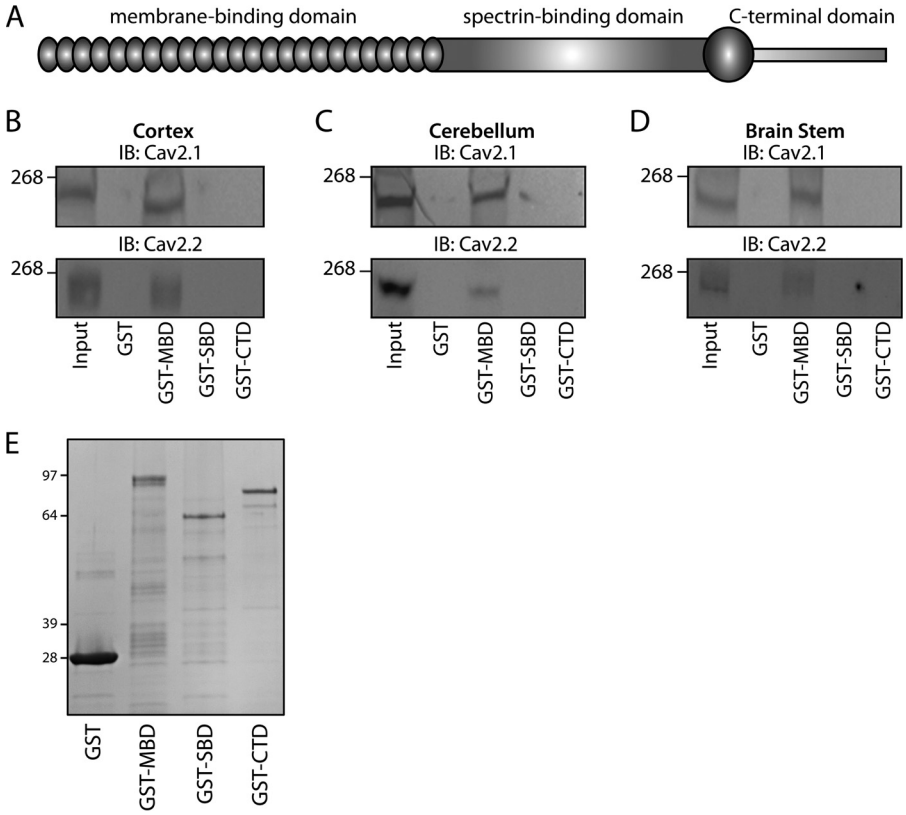

FIGURE 5. **Ankyrin-B associates with $Ca_v2.1$ and $Ca_v2.2$.** *A*, ankyrin-B comprises a membrane-binding domain, spectrin-binding domain, and a C-terminal regulatory domain. *B–D*, GST-ankyrin-B MBD associates with both $Ca_v2.1$ and $Ca_v2.2$ from detergent-soluble lysates of cortex (*B*), cerebellum (*C*), and brain stem (*D*). No interaction was observed between lysates and GST-ankyrin-B SBD, GST-ankyrin-B CTD, or GST alone. *E*, GST fusion proteins were utilized for pull-down experiments. Fusion proteins were purified from bacteria and analyzed by Coomassie Blue staining. Whereas GST migrates at 29 kDa, GST-ankyrin-B MBD migrates at 94 kDa. GST-ankyrin-B SBD migrates at 62 kDa, and GST-ankyrin-B CTD migrates at 79 kDa.

of both $Ca_v2.1$ and $Ca_v2.2$ expression in response to the reduction in ankyrin-B expression (Fig. 2).

Ankyrin-G Is Not Required for $Ca_v2.1$ or $Ca_v2.2$ Expression—Although encoded from different genes, ankyrin-B and ankyrin-G display similar domain organization, and both target ion channels and transporters in diverse excitable cell types (2). As both ankyrin-B and ankyrin-G are co-expressed in cell types harboring $Ca_v2.1$ and $Ca_v2.2$, we evaluated whether ankyrin-G is required for $Ca_v2.1$ and $Ca_v2.2$ expression as shown for ankyrin-B (Figs. 1 and 2). In contrast to findings for ankyrin-B-deficient tissue, we observed no difference in $Ca_v2.1$ or $Ca_v2.2$ expression in cerebellar lysates generated from a well characterized mouse model homozygous for a null mutation in cerebellar ankyrin-G (Fig. 3 and Ref. 20). These data demonstrate that ankyrin-B, but not ankyrin-G, is required for regulating $Ca_v2.1$ and $Ca_v2.2$ expression in the cerebellum. Moreover, these data suggest that ankyrins-G and -B play nonredundant roles in calcium channel targeting in brain.

Ankyrin-B Associates with $Ca_v2.1$ and $Ca_v2.2$ in Brain—Considering that $Ca_v2.1$ and $Ca_v2.2$ expression levels were significantly reduced in ankyrin-$B^{+/-}$ brain tissue (Figs. 1 and 2), we evaluated the ability of ankyrin-B to associate with $Ca_v2.1$ and $Ca_v2.2$ in brain. Co-IP analysis using detergent-soluble lysates from adult mouse cortex, cerebellum, and brain stem demonstrated that affinity-purified anti-$Ca_v2.1$ Ig co-immunoprecipitated ankyrin-B from cortex (Fig. 4*A*), cerebellum (Fig. 4*B*), and brain stem (Fig. 4*C*). Likewise, anti-$Ca_v2.2$ Ig co-immunoprecipitated ankyrin-B from cortex, cerebellum, and brain stem lysates (Fig. 4, *D–F*). We observed no interaction between ankyrin-B and control Ig in any tissue lysate (Fig. 4, *A–F*). To confirm this interaction, we performed reciprocal co-immunoprecipitations utilizing affinity-purified ankyrin-B Ig. Ankyrin-B Ig co-immunoprecipitated $Ca_v2.1$ and $Ca_v2.2$ from detergent-soluble lysates from cortex, cerebellum, and brain stem, whereas we observed no interaction with a control Ig (Fig. 4, *G–L*). Collectively, these data support an *in vivo* interaction between ankyrin-B and $Ca_v2.1$, as well as an *in vivo* interaction between ankyrin-B and $Ca_v2.2$, in mouse cortex, cerebellum, and brain stem.

We further evaluated the neuronal ankyrin-B/$Ca_v2.1$ and ankyrin-B/$Ca_v2.2$ interactions using pulldown experiments from mouse detergent-soluble cortex, cerebellum, and brain stem lysates. Ankyrin-B comprises three distinct structural domains: MBD, SBD, and CTD (Fig. 5*A*). Of note, GST-ankyrin-B MBD, but neither GST-ankyrin-B SBD or GST-ankyrin-B CTD interacted with $Ca_v2.1$ nor $Ca_v2.2$ from cortex (Fig. 5*B*), cerebellum (Fig. 5*C*), and brain stem (Fig. 5*D*; fusion proteins are shown in Fig. 5*E*). Collectively, these data demonstrate an interaction between $Ca_v2.1$ and $Ca_v2.2$ and ankyrin-B within multiple regions of the brain. These data further identify the structural requirements on ankyrin-B for Ca_v channel binding as the *ANK* repeats of the membrane-binding domain.

Ankyrin-B Interacts with the $Ca_v2.1$ and $Ca_v2.2$ DII/III Loops—Next, we evaluated the requirements on $Ca_v2.1$ and $Ca_v2.2$ for neuronal ankyrin-B binding. Previous studies have

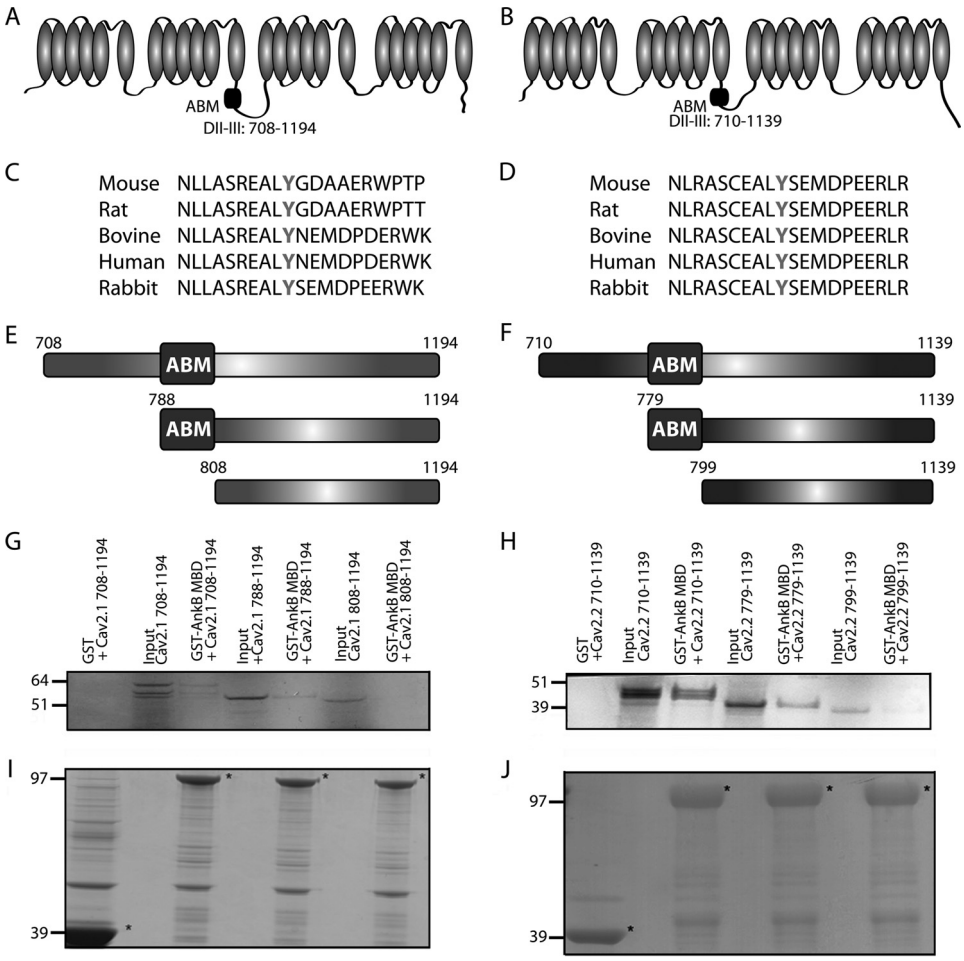

FIGURE 6. **$Ca_v2.1$ and $Ca_v2.2$ DII/DIII motif associates with ankyrin-B.** *A* and *B*, location of putative ABM in the DII/DIII cytoplasmic loop of $Ca_v2.1$ and $Ca_v2.2$ is shown. *C* and *D*, the putative ABM in $Ca_v2.1$ and $Ca_v2.2$ is conserved across species and harbors a central conserved tyrosine (*bolded*). *E* and *F*, three constructs were designed to evaluate the role of this amino acid sequence in ankyrin-B binding. These constructs include the entire DII/III loop, a portion of the loop that begins just prior to the putative ABM, and a portion of the loop that begins just after the putative ABM. *G* and *H*, *in vitro* binding assays demonstrate that, whereas the full-length DII/III loops of $Ca_v2.1$ and $Ca_v2.2$ and the smaller loop portion that contains the putative ABM are able to associate with GST-ankyrin-B MBD, the smaller loop portion that lacks this domain demonstrates no binding with GST-ankyrin-B MBD. *I* and *J*, Coomassie Blue staining demonstrating that equal loading of GST constructs was performed prior to imaging (denoted by *asterisks*).

suggested that a region in the DII/III loop region of $Ca_v2.2$ contains a region postulated to play a role in the targeting of calcium channels (34) (Fig. 6, *A* and *B*). This DII/III region contains a 20-amino acid motif that is highly conserved among species (Fig. 6, *C* and *D*). Three constructs based on $Ca_v2.1$ and $Ca_v2.2$ sequences were designed to evaluate the role of this motif in ankyrin-B/$Ca_v2.1$ and ankyrin-B/$Ca_v2.2$ association (Fig. 6, *E* and *F*). The first construct encompassed the entire DII/III loop ($Ca_v2.1$ amino acids 708–1194; $Ca_v2.2$ amino acids 710–1139); the second initiated proximal to the putative ankyrin-binding motif (ABM; $Ca_v2.1$ amino acids 788–1194; $Ca_v2.2$ amino acids 779–1139); and the third began distal to the ABM ($Ca_v2.1$ amino acids 808–1194; $Ca_v2.2$ amino acids 799–1139). *In vitro* binding with immobilized GST-ankyrin-B MBD revealed that the full-length $Ca_v2.1$ DII/III loop and the $Ca_v2.1$ construct containing residues 788–1194 displayed binding activity for GST-ankyrin-B MBD (Fig. 6*G*). In contrast, the $Ca_v2.1$ construct lacking residues 788–808 (construct 808–1194) had binding activity similar to GST alone (Fig. 6*G*). Similarly, full-length $Ca_v2.2$ DII/III loop and the $Ca_v2.2$ construct containing residues 779–799 (construct 779–1139) displayed binding activity for GST-ankyrin-B MBD (Fig. 6*H*). The $Ca_v2.2$ construct lacking residues 779–799 (construct 799–1139) had binding activity similar to GST alone (Fig. 6*H*). These data identify a 20-amino acid motif in both the $Ca_v2.1$ and $Ca_v2.2$ DII/III loops that is necessary for interaction with ankyrin-B.

A Conserved Tyrosine Residue Regulates Association with Ankyrin-B—Although inhibition of calcium channels is voltage-dependent, it is mediated by direct interaction of G protein $\beta\gamma$ subunits with the $\alpha 1$ pore-forming subunit of the channel (35, 36). Additionally, phosphorylation by tyrosine kinases has been shown to inhibit calcium channels (37) with G protein-dependent inhibition of calcium current due in part to a decrease in the open probability of the channel, resulting in reduced current density (38–40). We had previously defined a 20-amino acid motif in the DII/III loops of $Ca_v2.1$ and $Ca_v2.2$ that associates with ankyrin-B (Fig. 6). Notably, this motif contains a conserved tyrosine residue. To evaluate the role of this tyrosine in the regulation of $Ca_v2.1$ and $Ca_v2.2$ association with ankyrin-B, we incorporated a Y797E mutation in the $Ca_v2.1$ DII/III loop and evaluated the effect on *in vitro* binding (Fig. 7*A*). Mutagenesis of the Tyr-797 residue to a glutamic acid resulted in loss of association with GST-

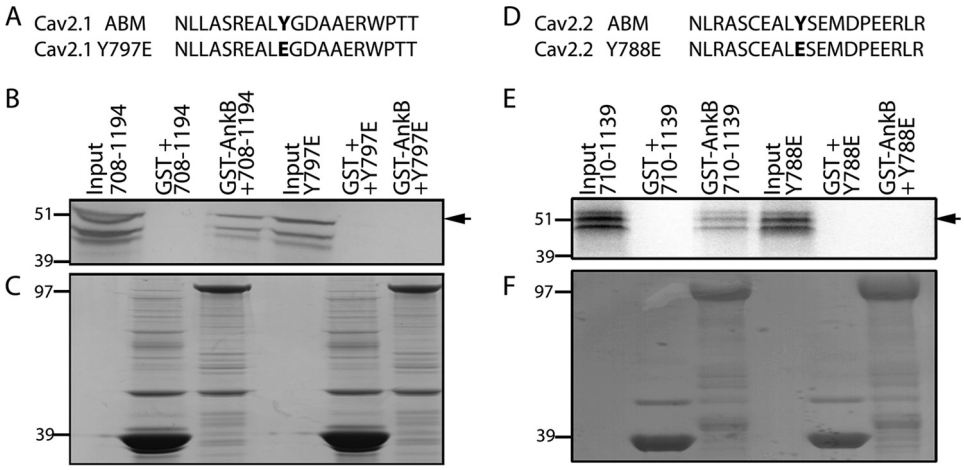

FIGURE 7. **A conserved tyrosine residue in the $Ca_v2.1$ and $Ca_v2.2$ DII/III loop is necessary for ankyrin-B interaction *in vitro*.** *A* and *D*, $Ca_v2.1$ and $Ca_v2.2$ DII/III loop domains contain a conserved tyrosine residue that was experimentally mutated to a glutamic acid to assess ankyrin-B binding. *B*, GST-ankyrin-B MBD was able to associate with the $Ca_v2.1$ DII/III loop domain. In contrast, there was a loss of interaction with the domain containing the Y797E mutation. There was no appreciable binding with GST alone. *E*, $Ca_v2.2$ DII/III loop domain associated with GST-ankyrin-B MBD is shown. However, there was no appreciable association between GST-ankyrin-B MBD and the $Ca_v2.2$ DII/III Y788E. There was no detectable binding to GST alone. *C* and *F*, Coomassie Blue stains demonstrate that equal loading of GST constructs was performed prior to imaging.

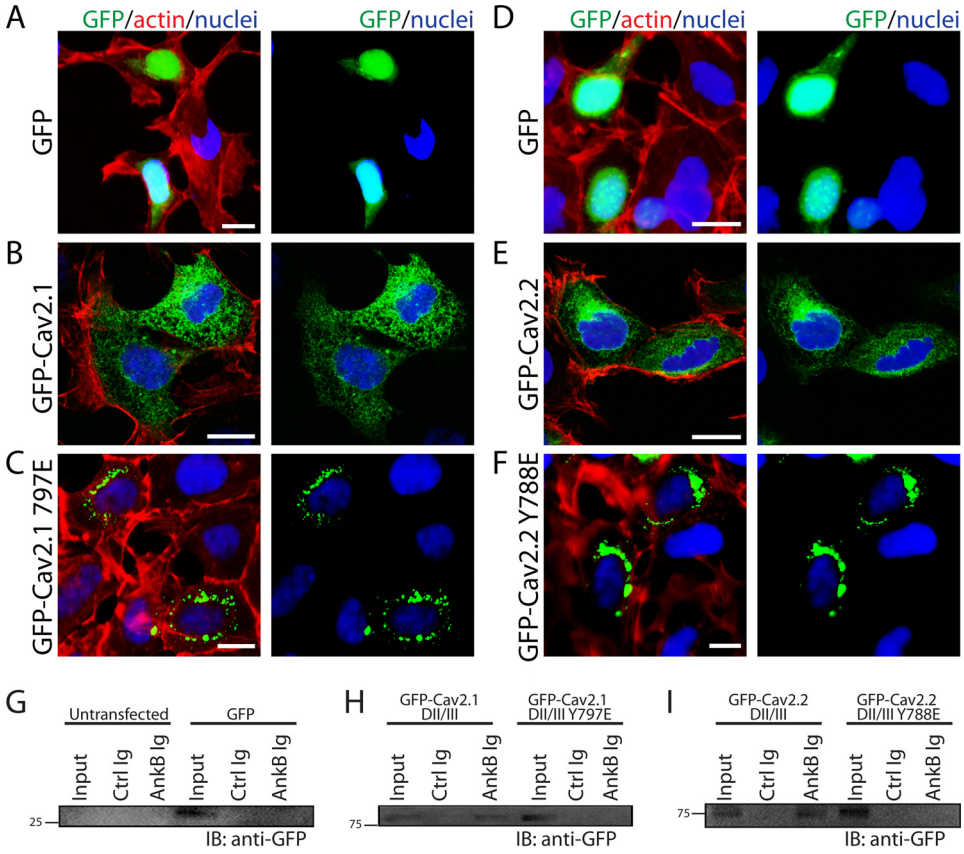

FIGURE 8. **$Ca_v2.1$/$Ca_v2.2$ tyrosine residues in ABM are critical for cellular targeting.** HEK293 cells transfected with pEGFP-C3 demonstrated a primarily nuclear localization pattern (*A* and *D*), whereas HEK293 cells transfected with $Ca_v2.1$ DII/III-GFP (*B*) or $Ca_v2.2$ DII/III-GFP (*E*) displayed a diffuse cellular pattern of expression unique from the nucleus. *C* and *F*, unlike WT constructs, both $Ca_v2.1$ Y797E-GFP and $Ca_v2.2$ Y788E-GFP were distributed in a tight perinuclear pattern. *Scale bars* denote 8 μm. *G–I*, a conserved tyrosine residue in the $Ca_v2.1$ and $Ca_v2.2$ DII/III loop is necessary for ankyrin-B interaction *in vitro*. *G*, in control experiments, ankyrin-B Ig did not interact with GFP alone expressed in HEK293 cells. *H* and *I*, ankyrin-B Ig co-immunoprecipitates GFP fusion protein containing the $Ca_v2.1$ or $Ca_v2.2$ DII/DII loop from transfected HEK293 cells. In contrast, ankyrin-B Ig does not co-immunoprecipitate GFP fusion proteins of $Ca_v2.1$ DII/DIII Y797E or $Ca_v2.2$ DII/III Y788E in parallel experiments. *IB*, immunoblotting.

ankyrin-B MBD by *in vitro* binding analysis (Fig. 7*B*). Mutation of the analogous residue, Tyr-788, in the $Ca_v2.2$ DII/III to a glutamic acid (Fig. 7*D*) demonstrated a similar loss of *in vitro* binding with GST-ankyrin-B MBD (Fig. 7*E*).

DII/DIII Tyrosine Residues Are Critical for $Ca_v2.1$/$Ca_v2.2$ Targeting—Ankyrin proteins are critical for targeting ion channels and transporters in diverse cell types including neurons. In fact, ion channel or transporter ankyrin-binding motifs alone

are sufficient to target GFP and other markers in heterologous cells and primary cultures (41). We therefore tested (i) whether the DII/DIII loops of $Ca_v2.1$ and $Ca_v2.2$ (that harbor ankyrin-binding motifs) were sufficient to behave as a dominant target signal in HEK293 cells, and (ii) whether the single tyrosine mutation in each channel altered this trafficking pattern. DII/DIII loops from $Ca_v2.1$ and $Ca_v2.2$ were subcloned in-frame into the pEGFP-C3 expression vector and transfected into HEK293 cells (express endogenous ankyrin-B). Confocal analysis revealed that unlike GFP that was exclusively found in the HEK293 cell nucleus (Fig. 8, *A* and *D*), GFP-$Ca_v2.1$ DII/III loop and GFP-$Ca_v2.2$ DII/III were in fact targeted outside of the nucleus (*versus* GFP) and had a diffuse pattern of expression throughout the cell (Fig. 8, *B* and *E*). Consistent with these findings, both GFP-$Ca_v2.1$ DII/III loop and GFP-$Ca_v2.2$ DII/III loop interacted with ankyrin-B in parallel co-IP experiments from transfected cells (Fig. 8, *G–I*). In contrast, GFP-$Ca_v2.1$ DII/III Y797E and GFP-$Ca_v2.2$ DII/III Y788E lacked ankyrin-B-binding activity (Fig. 8, *G–I*) and were restricted in localization to a tight and consistent perinuclear distribution (Fig. 8, *C* and *F*). These data demonstrate that the $Ca_v2.1$ and $Ca_v2.2$ DII/DIII loops harbor dominant targeting motifs that divert them from the nucleus. Further, these data implicate the Tyr-797 in the $Ca_v2.1$ and the Tyr-788 residue in the $Ca_v2.2$ as critical components in the regulation of calcium channel targeting.

We confirmed these findings in the context of full-length $Ca_v2.1$ and $Ca_v2.2$. We observed both GFP-$Ca_v2.1$ and GFP-$Ca_v2.2$ with diffuse expression across transfected HEK293 cells, whereas GFP-$Ca_v2.1$ Y797E and full-length GFP-$Ca_v2.2$ Y788E displayed abnormal targeting with a clustered perinuclear distribution (Fig. 9, *A–E*). Consistent with these findings, whereas GFP-$Ca_v2.1$ and GFP-$Ca_v2.2$ associated with ankyrin-B in co-IP experiments, ankyrin-B Ig was unable to co-immunoprecipitate either full-length GFP-$Ca_v2.1$ Y797E or full-length GFP-$Ca_v2.2$ Y788E from HEK293 cell lysates (Fig. 9, *F–H*). These results further support a critical role for ankyrin-B-mediated $Ca_v2.1$ and $Ca_v2.2$ expression and targeting.

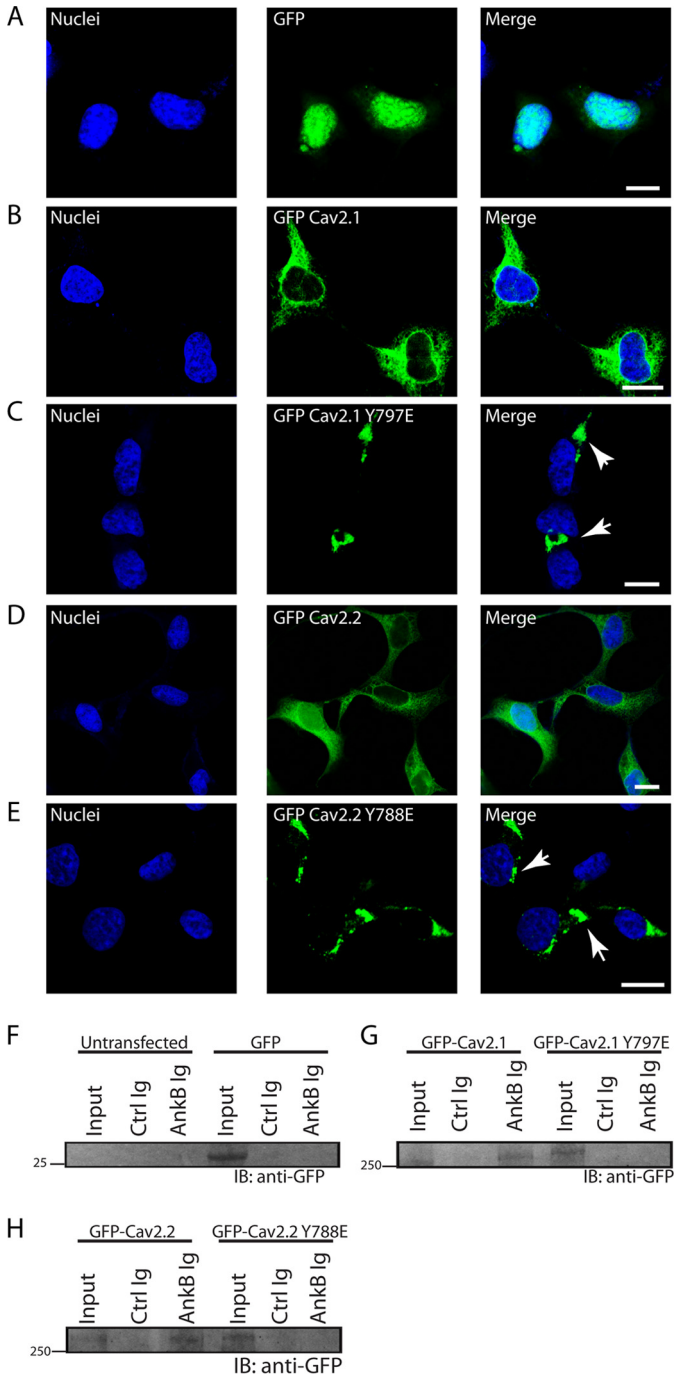

FIGURE 9. **$Ca_v2.1$/$Ca_v2.2$ tyrosine residues in ABM are critical for cellular targeting and ankyrin interaction.** *A*, HEK293 cells transfected with pEGFP-C3 demonstrated a primarily nuclear localization pattern. *B* and *D*, in contrast, HEK293 cells transfected with full-length GFP-$Ca_v2.1$ (*B*) or GFP-$Ca_v2.2$ (*D*) displayed a diffuse cellular pattern of expression unique from the nucleus or perinuclear region. *C* and *E*, unlike WT $Ca_v2.1$ and $Ca_v2.2$ constructs, both full-length GFP-$Ca_v2.1$ Y797E and full-length GFP-$Ca_v2.2$ Y788E-GFP were distributed in a tight perinuclear pattern (*white arrowheads*). *Scale bars* denote 8 μm. *F*, control experiments demonstrate that ankyrin-B Ig does not associate with GFP alone. *G*, ankyrin-B co-immunoprecipitates full-length GFP-$Ca_v2.1$, but not full-length GFP-$Ca_v2.1$ Y797E from transfected HEK293 lysates. *H*, ankyrin-B co-immunoprecipitates full-length GFP-$Ca_v2.2$, but not full-length GFP-$Ca_v2.2$ Y788E from transfected HEK293 lysates.

DISCUSSION

Our findings demonstrate a role of ankyrin-B for $Ca_v2.1$ and $Ca_v2.2$ channel expression and targeting in brain. Loss of ankyrin-B results in decreased expression of $Ca_v2.1$ and $Ca_v2.2$ in cortex, cerebellum, and brain stem. Moreover, mutation of a single residue in the $Ca_v2.1$ and $Ca_v2.2$ DII/III loop results in loss of association with ankyrin-B and abnormal cellular targeting. Ankyrin-B has been demonstrated to play a critical role in the establishment and maintenance of excitable domains in brain. Loss of ankyrin-B in mice results in significant nervous system defects, including hypoplasia of the corpus callosum and pyramidal tracts, dilation of the lateral ventricles, and deterioration of long axon tracts (25). Specifically, these phenotypes are associated with loss of L1CAM proteins throughout the brain. Interestingly, mutations in the human *L1CAM* gene cause mental retardation as well as a collection of neurological symptoms referred to as CRASH syndrome (corpus callosum hypoplasia, retardation, aphasia, spastic paraplegia, and hydrocephalus) (42). The ankyrin-$B^{-/-}$ mouse model, although lethal at post-natal day 1, exhibits loss of L1CAM from axons and exhibits many of the CRASH symptoms, although with greater severity (25). No humans with null mutations in the ankyrin-B gene (*ANK2*) have been identified; however, given

that heterozygote individuals with loss-of-function mutations in the *ANK2* gene are present in the population (43) and are found in patients with cardiac arrhythmia phenotypes (26, 44–47), it is possible that rare homozygous or mixed heterozygotes may exhibit CRASH symptoms. S1224L and Y1229H mutations in the human *L1CAM* gene are associated with CRASH syndrome (48). Moreover, these mutations are located within the highly conserved ankyrin-binding site and abolish association of L1 with ankyrin-B (48).

$Ca_v2.1$ and $Ca_v2.2$ channel activity in brain is necessary for proper initiation of synaptic transmission. $Ca_v2.2^{-/-}$ animals demonstrate normal motor coordination; however, these mice exhibit reduced responses to pain stimuli (49) and elevated aggression (50). $Ca_v2.1^{-/-}$ animals demonstrate dystonia at postnatal day 10–12 and rarely survive past weaning (51). Likewise, $Ca_v2.1^{-/-}$ mice exhibit reduced responses to pain stimuli (52). As noted above, ankyrin-$B^{-/-}$ die at birth, therefore we currently lack data on the *in vivo* phenotypes of ankyrin-B deficiency in an adult mouse. Future studies utilizing inducible ankyrin-B knock-out strategies in the postnatal mouse will be important for understanding the role of this cytoskeletal protein in synaptic function.

Finally, although our data link ankyrin-B with regulation of targeting via the DII/DIII loop of both $Ca_v2.1$ and $Ca_v2.2$ via specific tyrosine residues, it is possible that other protein interactions in this loop may also play critical roles in ion channel processing and membrane regulation. For example, the $Ca_v2.2$ DII/DIII loop maintains a SNARE binding or synprint region that has been linked with Ca_v channel targeting (34). It will be important in future work to understand the potential dual regulation of Ca_v channel targeting by ankyrin and other proteins.

REFERENCES

1. Cheever, T. R., and Ervasti, J. M. (2013) Actin isoforms in neuronal development and function. *Int. Rev. Cell Mol. Biol.* **301,** 157–213
2. Bennett, V., and Healy, J. (2008) Organizing the fluid membrane bilayer: diseases linked to spectrin and ankyrin. *Trends Mol. Med.* **14,** 28–36
3. Dunlap, K., Luebke, J. I., and Turner, T. J. (1995) Exocytotic Ca^{2+} channels in mammalian central neurons. *Trends Neurosci.* **18,** 89–98
4. Catterall, W. A. (2000) Structure and regulation of voltage-gated Ca^{2+} channels. *Annu. Rev. Cell Dev. Biol.* **16,** 521–555
5. Clapham, D. E. (1995) Calcium signaling. *Cell* **80,** 259–268
6. Snutch, T. P., and Reiner, P. B. (1992) Ca^{2+} channels: diversity of form and function. *Curr. Opin. Neurobiol.* **2,** 247–253
7. Tedford, H. W., and Zamponi, G. W. (2006) Direct G protein modulation of Ca_v2 calcium channels. *Pharmacol. Rev.* **58,** 837–862
8. Tsien, R. W., Lipscombe, D., Madison, D. V., Bley, K. R., and Fox, A. P. (1988) Multiple types of neuronal calcium channels and their selective modulation. *Trends Neurosci.* **11,** 431–438
9. Miller, R. J. (1997) Calcium channels prove to be a real headache. *Trends Neurosci.* **20,** 189–192
10. Ellinor, P. T., Zhang, J. F., Randall, A. D., Zhou, M., Schwarz, T. L., Tsien, R. W., and Horne, W. A. (1993) Functional expression of a rapidly inactivating neuronal calcium channel. *Nature* **363,** 455–458
11. Fox, A. P., Nowycky, M. C., and Tsien, R. W. (1987) Kinetic and pharmacological properties distinguishing three types of calcium currents in chick sensory neurones. *J. Physiol.* **394,** 149–172
12. Usowicz, M. M., Sugimori, M., Cherksey, B., and Llinás, R. (1992) P-type calcium channels in the somata and dendrites of adult cerebellar Purkinje cells. *Neuron* **9,** 1185–1199
13. Wheeler, D. B., Randall, A., and Tsien, R. W. (1994) Roles of N-type and Q-type Ca^{2+} channels in supporting hippocampal synaptic transmission. *Science* **264,** 107–111
14. Takahashi, T., and Momiyama, A. (1993) Different types of calcium channels mediate central synaptic transmission. *Nature* **366,** 156–158
15. Nooney, J. M., and Lodge, D. (1996) The use of invertebrate peptide toxins to establish Ca^{2+} channel identity of CA3-CA1 neurotransmission in rat hippocampal slices. *Eur. J. Pharmacol.* **306,** 41–50
16. Olivera, B. M., Miljanich, G. P., Ramachandran, J., and Adams, M. E. (1994) Calcium channel diversity and neurotransmitter release: the ω-conotoxins and ω-agatoxins. *Annu. Rev. Biochem.* **63,** 823–867
17. Leroy, J., Richards, M. S., Butcher, A. J., Nieto-Rostro, M., Pratt, W. S., Davies, A., and Dolphin, A. C. (2005) Interaction via a key tryptophan in the I-II linker of N-type calcium channels is required for $\beta1$ but not for palmitoylated $\beta2$, implicating an additional binding site in the regulation of channel voltage-dependent properties. *J. Neurosci.* **25,** 6984–6996
18. Davies, A., Hendrich, J., Van Minh, A. T., Wratten, J., Douglas, L., and Dolphin, A. C. (2007) Functional biology of the $\alpha_2\delta$ subunits of voltage-gated calcium channels. *Trends Pharmacol. Sci.* **28,** 220–228
19. Bennett, V., and Baines, A. J. (2001) Spectrin and ankyrin-based pathways: metazoan inventions for integrating cells into tissues. *Physiol. Rev.* **81,** 1353–1392
20. Zhou, D., Lambert, S., Malen, P. L., Carpenter, S., Boland, L. M., and Bennett, V. (1998) Ankyrin-G is required for clustering of voltage-gated Na channels at axon initial segments and for normal action potential firing. *J. Cell Biol.* **143,** 1295–1304
21. Jenkins, S. M., and Bennett, V. (2001) Ankyrin-G coordinates assembly of the spectrin-based membrane skeleton, voltage-gated sodium channels, and L1 CAMs at Purkinje neuron initial segments. *J. Cell Biol.* **155,** 739–746
22. Pan, Z., Kao, T., Horvath, Z., Lemos, J., Sul, J. Y., Cranstoun, S. D., Bennett, V., Scherer, S. S., and Cooper, E. C. (2006) A common ankyrin-G-based mechanism retains KCNQ and Na_V channels at electrically active domains of the axon. *J. Neurosci.* **26,** 2599–2613
23. Ango, F., di Cristo, G., Higashiyama, H., Bennett, V., Wu, P., and Huang, Z. J. (2004) Ankyrin-based subcellular gradient of neurofascin, an immunoglobulin family protein, directs GABAergic innervation at Purkinje axon initial segment. *Cell* **119,** 257–272
24. Galiano, M. R., Jha, S., Ho, T. S., Zhang, C., Ogawa, Y., Chang, K. J., Stankewich, M. C., Mohler, P. J., and Rasband, M. N. (2012) A distal axonal cytoskeleton forms an intra-axonal boundary that controls axon initial segment assembly. *Cell* **149,** 1125–1139
25. Scotland, P., Zhou, D., Benveniste, H., and Bennett, V. (1998) Nervous system defects of ankyrin-$B^{-/-}$ mice suggest functional overlap between the cell adhesion molecule L1 and 440-kD ankyrin-B in premyelinated axons. *J. Cell Biol.* **143,** 1305–1315
26. Le Scouarnec, S., Bhasin, N., Vieyres, C., Hund, T. J., Cunha, S. R., Koval, O., Marionneau, C., Chen, B., Wu, Y., Demolombe, S., Song, L. S., Le Marec, H., Probst, V., Schott, J. J., Anderson, M. E., and Mohler, P. J. (2008) Dysfunction in ankyrin-B-dependent ion channel and transporter targeting causes human sinus node disease. *Proc. Natl. Acad. Sci. U.S.A.* **105,** 15617–15622
27. Cunha, S. R., Hund, T. J., Hashemi, S., Voigt, N., Li, N., Wright, P., Koval, O., Li, J., Gudmundsson, H., Gumina, R. J., Karck, M., Schott, J. J., Probst, V., Le Marec, H., Anderson, M. E., Dobrev, D., Wehrens, X. H., and Mohler, P. J. (2011) Defects in ankyrin-based membrane protein targeting pathways underlie atrial fibrillation. *Circulation* **124,** 1212–1222
28. Abdi, K. M., Mohler, P. J., Davis, J. Q., and Bennett, V. (2006) Isoform specificity of ankyrin-B: a site in the divergent C-terminal domain is required for intramolecular association. *J. Biol. Chem.* **281,** 5741–5749
29. Cunha, S. R., Bhasin, N., and Mohler, P. J. (2007) Targeting and stability of Na/Ca exchanger 1 in cardiomyocytes requires direct interaction with the membrane adaptor ankyrin-B. *J. Biol. Chem.* **282,** 4875–4883
30. Cunha, S. R., and Mohler, P. J. (2008) Obscurin targets ankyrin-B and protein phosphatase 2A to the cardiac M-line. *J. Biol. Chem.* **283,** 31968–31980
31. Westenbroek, R. E., Sakurai, T., Elliott, E. M., Hell, J. W., Starr, T. V., Snutch, T. P., and Catterall, W. A. (1995) Immunochemical identification and subcellular distribution of the α_{1A} subunits of brain calcium channels. *J. Neurosci.* **15,** 6403–6418

32. Indriati, D. W., Kamasawa, N., Matsui, K., Meredith, A. L., Watanabe, M., and Shigemoto, R. (2013) Quantitative localization of $Ca_v2.1$ (P/Q-type) voltage-dependent calcium channels in Purkinje cells: somatodendritic gradient and distinct somatic coclustering with calcium-activated potassium channels. *J. Neurosci.* **33,** 3668–3678
33. Kordeli, E., Davis, J., Trapp, B., and Bennett, V. (1990) An isoform of ankyrin is localized at nodes of Ranvier in myelinated axons of central and peripheral nerves. *J. Cell Biol.* **110,** 1341–1352
34. Mochida, S., Westenbroek, R. E., Yokoyama, C. T., Zhong, H., Myers, S. J., Scheuer, T., Itoh, K., and Catterall, W. A. (2003) Requirement for the synaptic protein interaction site for reconstitution of synaptic transmission by P/Q-type calcium channels. *Proc. Natl. Acad. Sci. U.S.A.* **100,** 2819–2824
35. Ikeda, S. R. (1996) Voltage-dependent modulation of N-type calcium channels by G-protein $\beta\gamma$ subunits. *Nature* **380,** 255–258
36. Herlitze, S., Garcia, D. E., Mackie, K., Hille, B., Scheuer, T., and Catterall, W. A. (1996) Modulation of Ca^{2+} channels by G-protein $\beta\gamma$ subunits. *Nature* **380,** 258–262
37. Dolphin, A. C. (2003) G protein modulation of voltage-gated calcium channels. *Pharmacol. Rev.* **55,** 607–627
38. Yue, D. T., Backx, P. H., and Imredy, J. P. (1990) Calcium-sensitive inactivation in the gating of single calcium channels. *Science* **250,** 1735–1738
39. Delcour, A. H., and Tsien, R. W. (1993) Altered prevalence of gating modes in neurotransmitter inhibition of N-type calcium channels. *Science* **259,** 980–984
40. Patil, P. G., de Leon, M., Reed, R. R., Dubel, S., Snutch, T. P., and Yue, D. T. (1996) Elementary events underlying voltage-dependent G-protein inhibition of N-type calcium channels. *Biophys. J.* **71,** 2509–2521
41. Garrido, J. J., Giraud, P., Carlier, E., Fernandes, F., Moussif, A., Fache, M. P., Debanne, D., and Dargent, B. (2003) A targeting motif involved in sodium channel clustering at the axonal initial segment. *Science* **300,** 2091–2094
42. Fransen, E., Van Camp, G., Vits, L., and Willems, P. J. (1997) L1-associated diseases: clinical geneticists divide, molecular geneticists unite. *Hum. Mol. Genet.* **6,** 1625–1632
43. Mohler, P. J., Healy, J. A., Xue, H., Puca, A. A., Kline, C. F., Allingham, R. R., Kranias, E. G., Rockman, H. A., and Bennett, V. (2007) Ankyrin-B syndrome: enhanced cardiac function balanced by risk of cardiac death and premature senescence. *PLoS ONE* **2,** e1051
44. Mohler, P. J., Le Scouarnec, S., Denjoy, I., Lowe, J. S., Guicheney, P., Caron, L., Driskell, I. M., Schott, J. J., Norris, K., Leenhardt, A., Kim, R. B., Escande, D., and Roden, D. M. (2007) Defining the cellular phenotype of "ankyrin-B syndrome" variants: human ANK2 variants associated with clinical phenotypes display a spectrum of activities in cardiomyocytes. *Circulation* **115,** 432–441
45. Mohler, P. J., Schott, J. J., Gramolini, A. O., Dilly, K. W., Guatimosim, S., duBell, W. H., Song, L. S., Haurogné, K., Kyndt, F., Ali, M. E., Rogers, T. B., Lederer, W. J., Escande, D., Le Marec, H., and Bennett, V. (2003) Ankyrin-B mutation causes type 4 long-QT cardiac arrhythmia and sudden cardiac death. *Nature* **421,** 634–639
46. Mohler, P. J., and Trafford, A. W. (2011) The devil is in the details: methodological reviews, a new JMCC initiative. *J. Mol. Cell. Cardiol.* **50,** 939
47. Sedlacek, K., Stark, K., Cunha, S. R., Pfeufer, A., Weber, S., Berger, I., Perz, S., Kääb, S., Wichmann, H. E., Mohler, P. J., Hengstenberg, C., and Jeron, A. (2008) Common genetic variants in ANK2 modulate QT interval: results from the KORA study. *Circ. Cardiovasc. Genet.* **1,** 93–99
48. Needham, L. K., Thelen, K., and Maness, P. F. (2001) Cytoplasmic domain mutations of the L1 cell adhesion molecule reduce L1-ankyrin interactions. *J. Neurosci.* **21,** 1490–1500
49. Kim, C., Jun, K., Lee, T., Kim, S. S., McEnery, M. W., Chin, H., Kim, H. L., Park, J. M., Kim, D. K., Jung, S. J., Kim, J., and Shin, H. S. (2001) Altered nociceptive response in mice deficient in the α_{1B} subunit of the voltage-dependent calcium channel. *Mol. Cell. Neurosci.* **18,** 235–245
50. Kim, C., Jeon, D., Kim, Y. H., Lee, C. J., Kim, H., and Shin, H. S. (2009) Deletion of N-type Ca^{2+} channel $Ca_v2.2$ results in hyperaggressive behaviors in mice. *J. Biol. Chem.* **284,** 2738–2745
51. Jun, K., Piedras-Rentería, E. S., Smith, S. M., Wheeler, D. B., Lee, S. B., Lee, T. G., Chin, H., Adams, M. E., Scheller, R. H., Tsien, R. W., and Shin, H. S. (1999) Ablation of P/Q-type Ca^{2+} channel currents, altered synaptic transmission, and progressive ataxia in mice lacking the α_{1A}-subunit. *Proc. Natl. Acad. Sci. U.S.A.* **96,** 15245–15250
52. Luvisetto, S., Marinelli, S., Panasiti, M. S., D'Amato, F. R., Fletcher, C. F., Pavone, F., and Pietrobon, D. (2006) Pain sensitivity in mice lacking the $Ca_v2.1\alpha1$ subunit of P/Q-type Ca^{2+} channels. *Neuroscience* **142,** 823–832